Intermittency in the Hodgkin-Huxley model

Gaspar Cano¹ and Rui Dilão^{1,2}

1-University of Lisbon, Instituto Superior Técnico, Av. Rovisco Pais, 1049-001 Lisbon, Portugal.

and

2-Institut des Hautes Études Scientifiques, 35, route de Chartres, 91440 Bures-sur-Yvette, France

E-mail: ruidilao@tecnico.ulisboa.pt

February 2016

Abstract. We show that action potentials in the Hodgkin-Huxley neuron model result from a type I intermittency phenomenon that occurs in the proximity of a saddle-node bifurcation of limit cycles. For the Hodgkin-Huxley spatially extended model, describing propagation of action potential along axons, we show the existence of type I intermittency and a new type of chaotic intermittency, as well as space propagating regular and chaotic diffusion waves. Chaotic intermittency occurs in the transition from a turbulent regime to the resting regime of the transmembrane potential and is characterised by the existence of a sequence of action potential spikes occurring at irregular time intervals.

Keywords: Hodgkin-Huxley neuron model, type I intermittency, chaotic intermittency, diffusion waves

1. Introduction

As nucleic acids are intrinsically negatively charged molecules, inside the cell, the zero charge balance is compensated by a non-zero concentration of positively charged ions. The transport of ions from the interior to the exterior of a cell and vice versa is done by ion channels and pumps. These channels and pumps are transmembrane proteins localised along the cellular membrane, [Keener and Sneyd, 1998].

Transmembrane channels and pumps are specific to the type of ion $(Na^+, K^+, Ca^{++}, etc.)$ and, at equilibrium, a potential difference V from the inside to the outside of the cell is kept. Inside the cell, the potential is lower when compared with the potential outside the cell. The exchange of ions from the interior to the exterior of the cell is due to two competing effects. One effect is related with the differences of concentrations in the two regions. The other effect is due to the electrostatic forces between charged ions.

The Hodgkin-Huxley (HH) neuron excitation model, [Hodgkin and Huxley, 1952], describes the potential drop across cell membranes due to the exchange of ions. This

model has been introduced to describe patch clamp experiments on the giant axon of the squid *Loligo*, [Hodgkin and Huxley, 1952b] and [Hodgkin and Huxley, 1952]. The equations of the HH model are

$$C_{m} \frac{\partial V}{\partial t} = \tilde{D} \frac{\partial^{2} V}{\partial x^{2}} - g_{\text{Na}} m^{3} h(V - V_{\text{Na}}^{N}) - g_{\text{K}} n^{4} (V - V_{\text{K}}^{N}) - g_{\text{L}} (V - V_{\text{L}}^{N}) + i$$

$$\frac{\partial n}{\partial t} = \alpha_{n}(V)(1 - n) - \beta_{n}(V) n = G_{n}(V, n)$$

$$\frac{\partial m}{\partial t} = \alpha_{m}(V)(1 - m) - \beta_{m}(V) m = G_{m}(V, m)$$

$$\frac{\partial h}{\partial t} = \alpha_{h}(V)(1 - h) - \beta_{h}(V) h = G_{h}(V, h),$$

$$(1)$$

where

$$\alpha_{n} = 0.01 \phi \frac{V + 10}{e^{(V+10)/10} - 1}, \quad \beta_{n} = 0.125 \phi e^{V/80},
\alpha_{m} = 0.1 \phi \frac{V + 25}{e^{(V+25)/10} - 1}, \quad \beta_{m} = 4 \phi e^{V/18},
\alpha_{h} = 0.07 \phi e^{V/20}, \qquad \beta_{h} = \phi \frac{1}{e^{(V+30)/10} - 1},
\phi = 3^{(T-6.3)/19}.$$
(2)

In this model, V is the transmembrane potential drop measured in mV, i is a transmembrane current, measured in μ A/cm² and time is measured in ms. The current i is a transmembrane current that is applied to the cell. For example, it can be an injected current in a patch clamp experiment, or the signal transmitted from other neurons through synapses.

Ion channels open and close as a function of the potential difference between the inside and outside of cells. The gating variables n, m and h describe the opening and closing of the channel gates, are specific to the ion type and are dimensionless. The functional form of n, m and h in equations (1) has been proposed and calibrated in [Hodgkin and Huxley, 1952]. For a review of specific gating mechanisms associated to the choices made in equation (1), we refer to [Keener and Sneyd, 1998].

In equations (1), the ionic conductances across the cellular membrane are g_{Na} and g_{K} , and g_{L} is a constant measuring "leak" conductance. C_m is the membrane capacitance and \tilde{D} is a constant inversely proportional to the resistance (Ω), measured along the axon of nerve cells. This model has been calibrated for the squid giant axon at the temperature T=6.3 °C, [Hodgkin and Huxley, 1952], and the values of the constants are $C_m=1~\mu\text{F/cm}^2$, $g_{\text{Na}}=120~\text{mS/cm}^2$, $g_{\text{K}}=36~\text{mS/cm}^2$ and $g_{\text{L}}=0.3~\text{mS/cm}^2$, where $S=\Omega^{-1}$ (siemens) is the unit of conductance. The Nernst equilibrium potentials, relating the difference in the concentrations of ions between the inside and the outside of cells with the transmembrane potential drop, are $V_{\text{Na}}^N=-115~\text{mV}$, $V_{\text{K}}^N=12~\text{mV}$ and $V_{\text{L}}^N=-10.613~\text{mV}$. This choice of parameters is rescaled in such a way that at rest (i=0), the steady state of the the transmembrane potential is $V^*(0)=0~\text{mV}$.

For $\tilde{D}=0$, the HH equations describe the potential drop across the walls of a globular cell and the ionic gradients inside the cell are negligible. Hodgkin and Huxley have shown that the transmembrane diffusion coefficient is $\tilde{D}=a/(2R_2)$, where a is the radius of the axon (considered as a cylinder) and R_2 is the specific resistivity along the interior of the axon. For the case of the squid giant axon, $a=238~\mu\text{m}$, $R_2=35.4~\Omega$ cm and $\tilde{D}=3.4\times10^{-4}~\text{S}$, [Hodgkin and Huxley, 1952].

The electrophysiological state of any cell can be described by a HH type model, provided its electric state is controlled by the opening and closing of voltage sensitive channels.

The success of the HH model in describing the dynamics of certain types of neurons relies on its ability to reproduce some experimental facts of patch-clamp experiments, including action potentials and threshold effects. To describe the electrophysiological state of a simple (globular) neuron or cell, we assume $\tilde{D}=0$ in equations (1). In this case, the electrophysiological steady state of the cell or neuron is described by the vector quantity $x^*(i) = (V^*(i), n^*(i), m^*(i), h^*(i))$, where i is considered as an external parameter. If i = 0, for the (reference) parameter values described above, the steady state is stable and it is the unique limit set of the HH equations (1).

As the position of the steady state $x^*(i)$ changes with i, due to the stability of the steady state $x^*(i)$ in the vicinity of i = 0, small variations in the parameter i for a short period of time produce the same dynamic effects as changes in the initial conditions. This simple fact about solutions of the HH equations for $\tilde{D} = 0$ and i = 0 implies that the electrophysiological state of the cell is characterised by $x^*(0)$. However, the solutions of the HH equations show a transient phenomenon called action potential. The main facts about the action potential and the associated threshold effect are the following:

- 1) Consider a cell or neuron at the steady state $x^*(0)$. Imposing a current to the cell during some short time t_1 , there exists a time interval Δt_{tr} and a threshold value I_{tr} such that, if $i(t) \geq I_{tr}$, for $\Delta t_{tr} \leq t \leq m\Delta t_{tr}$, with finite real m > 1, and i(t) = 0 otherwise, the system develops a spike in its voltage response V(t) the action potential. Then the voltage attenuates in time and the system returns to the stable steady state $x^*(0)$. If $i(t) < I_{tr}$, for $\Delta t_{tr} \leq t \leq m\Delta t_{tr}$, the voltage response V(t) attenuates in time to the stable steady state $x^*(0)$ and the action potential does not develop.
- 2) Perturbing the HH equations (1) with a sequence of current rectangular pulses above threshold I_{tr} , and if the temporal differences between pulses are above some time interval Δt_r , then the solutions of the HH equations develop the same number of pulses as in the current exciting signal. We call Δt_r the refractory interval. If we perturb continuously the HH model with a current made of a sequence of rectangular pulses above threshold, and the temporal distance between pulses is below the refractory interval Δt_r , then the number of pulses in the voltage response is smaller than the number of pulses of the exciting signal.

In figure 1, we show the voltage response in a globular neuron $(\tilde{D}=0)$ to a

long current perturbation and to a square wave type perturbation. These two solutions illustrate the properties of the transient behaviour as explained in the two cases described above. For the numerical simulations of equations (1), with the steady state $x^*(0)$ as initial condition, the threshold parameters are $I_{tr} \simeq 2.25 \ \mu\text{A/cm}^2$, $\Delta t_{tr} \simeq 1.5 \ \text{ms}$ and the refractory period is $\Delta t_r \simeq 17.5 \ \text{ms}$.

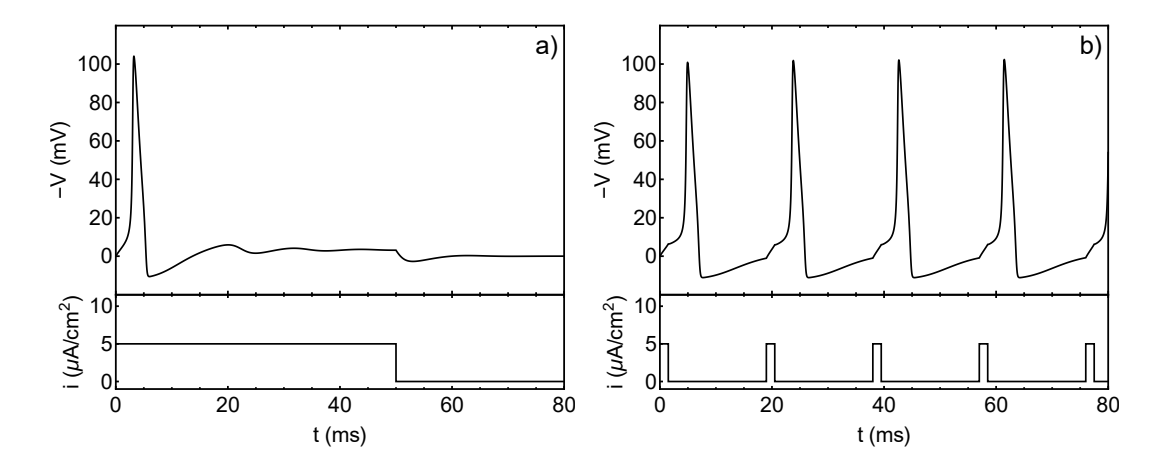


Figure 1. a) Voltage response of the HH equations (1) as a function of time, for the stimulation signal $i(t)=5>I_{tr}$, for $t\in[0,50]$, and i(t)=0 otherwise — threshold property 1). In b), we perturbed the cell with a square wave, with a time difference between spikes $\Delta t=17.5$ ms — property 2). For the parameter values of the simulations, $I_{tr}=2.25~\mu\text{A/cm}^2$, $\Delta t_{tr}\simeq1.5$ ms and the refractory interval is $\Delta t_r\simeq17.5$ ms.

For the parameter region of the simulations in figure 1, the HH equations have a unique stable steady state (stable node) in the four dimensional phase space. These simple facts are well known and discussed in the literature, [Rinzel and Miller, 1980], [Izhikevich, 2007] and [Ermentrout and Terman, 2010], among others.

One of the main goals of this paper is to explain the origin of the threshold effect and the appearance of action potential spikes in the HH model equations and to characterise it dynamically. In the next section, we summarise the main dynamical properties of the solutions of the diffusion free $(\tilde{D}=0)$ HH equations (1). It is shown that, for the parameter values described above and bifurcation parameter i, the HH equations (1) have a codimension 2 Bautin bifurcation scenario. Upon variation of the bifurcation parameter i, this bifurcation scenario has a subcritical and a supercritical Hopf bifurcation and a global saddle-node bifurcation of limit cycles. In section 3, we extend the concept of type I intermittency associated to saddle-node bifurcations of fixed points to intermittency of saddle-node bifurcation of limit cycles. We derive the scaling properties of this new type of intermittency. We show that action potentials, as observed in the HH equation, are originated by this new type I intermittency. In section 4, we analyse the spatially extended HH model $(\tilde{D}>0)$ and show that a new type I intermittency appears, responsible for the propagation of the action potentials along the axon. In the presence of diffusion, sustained oscillations develop, as well as chaotic

or turbulent action potential propagation. For high values of transmembrane currents, turbulent action potentials disappear and the convergence to a stable steady state occurs mixed with intermittent action potential chaotic spikes. We call chaotic intermittency to this new kind of intermittency of the HH extended model. Intermittency effects in neuronal systems have been reported by several authors, [Rae-Grant and Kim, 1994] and [Velazquez et al., 1999]. Finally, in section 5, we summarise the main conclusions of this paper.

2. A summary of the bifurcations of the diffusion free HH equation

For the diffusion free HH equations (1), the basic properties of its solutions are well known and the basic phase space structure is also well known. In this analysis, all the parameters of equations (1) are kept fixed and the current i is considered as the unique free parameter of the model. The basic analysis includes the numerical simulations of the time responses, topology of orbits in the 4 dimensional phase space, bifurcation analysis of fixed points and the possible existence of chaotic behaviour in a restricted parameter region of the model. The basic bifurcation analysis of fixed points as a function of i, including the existence of two Hopf bifurcations of fixed points, one subcritical and another supercritical, has been exhaustively analysed in [Hassard, 1978] and [Rinzel and Miller, 1980]. The existence of chaotic behaviour has been explored in [Guckenheimer and Oliva, 2002] in a very narrow region of the parameter i. A period doubling effect on the period of limit cycles has been reported in [Hassard, 1978] and [Rinzel and Miller, 1980], however this effect is not a period doubling codimension 1 bifurcation. For a review, recent references are [Izhikevich, 2007] and [Ermentrout and Terman, 2010]. The majority of authors have done the numerical analysis of the HH equations (1) with the bifurcation analysis software AUTO, [Doedel et al., 1991], and XPPAUT, [Ermentrout, 2002].

The bifurcation diagram depicted in figure 2 summarises the main characteristics of the asymptotic solutions of the diffusion free HH equations ($\tilde{D}=0$). The HH equations (1) have a unique fixed point with coordinates $x^*(i)=(V^*(i),n^*(i),m^*(i),h^*(i))$, whose position in phase space depends on i (the other parameters in (1) are kept fixed). The fixed point $x^*(i)$ has two Hopf bifurcations, one subcritical for $i=I_1$, and another supercritical for $i=I_2$. For $i>I_2$ and $0 \le i < I_1$, the fixed point $x^*(i)$ is stable. For the parameter values in equations (1), $I_1=9.77$ and $I_2=154.52$. The local bifurcation analysis shows that for $i<I_1$ and I_1-i sufficiently small, the HH equations have at least two limit cycles, one stable and another unstable, [Hassard, 1978] and [Rinzel and Miller, 1980]. The unstable limit cycle is created at I_1 , for decreasing values of i, and the stable one is created at I_2 , also for decreasing values of i. These two limit cycles collide at $i=I_0 < I_1$ and, for $i < I_0$ they do not exist. At $i=I_0=6.26$, the HH equation has a saddle-node limit cycle bifurcation (SNLC), [Kuznetsov, 2004]. In this analysis, we have considered the fixed reference temperature T=6.3 °C. However, for temperature T below 28.8 °C, the overall behaviour of the

bifurcation diagram is the same as the one in figure 2.

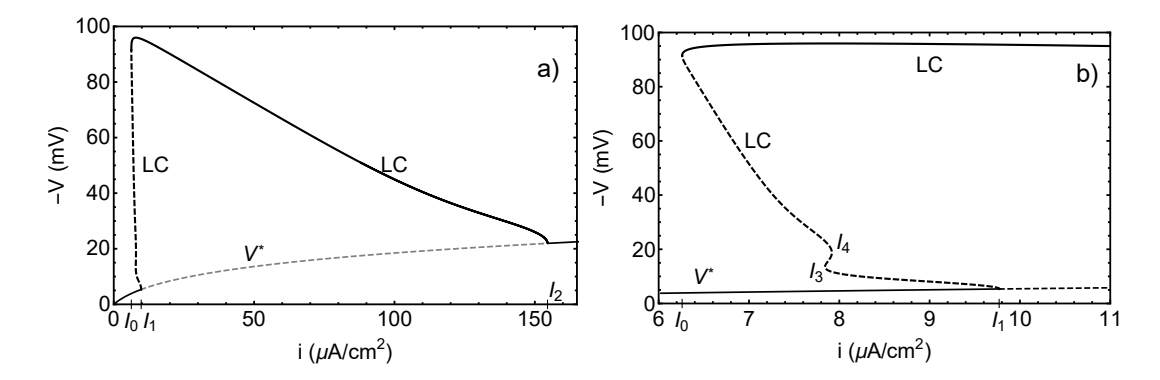


Figure 2. a) Bifurcation diagram for the diffusion free HH equations (1) as a function of the transmembrane current parameter i. In the bifurcation diagram, we represent the stability of the coordinate $V^*(i)$ of the fixed point $x^*(i)$ and the maximum values of the V(i)-coordinate of the limit cycles (LC) associated with the Hopf bifurcations. Dotted lines correspond to unstable states and continuous lines to stable ones. The SNLC bifurcation occurs for $i = I_0 = 6.26$, the subcritical Hopf bifurcation for $i = I_1 = 9.77$ and the supercritical Hopf bifurcation for $i = I_2 = 154.52$. b) Enlargement of the region in the neighbourhood of the "knee" that occurs in the interval $[I_3, I_4] = [7.84, 7.92]$. The bifurcation diagrams have been calculated with the software packages AUTO and XPPAUT.

The fixed point $x^*(i)$ is unstable for i in the interior of the interval $[I_1, I_2]$ and stable outside. Away from the bifurcation points, the fixed point $x^*(i)$ is hyperbolic. The overall behaviour of the bifurcation diagram in figure 2a) can be understood as a codimension 2 Bautin or generalised Hopf bifurcation, [Kuznetsov, 2004]. We assume that the "knee" (figure 2b) and [Rinzel and Miller, 1980]) of the bifurcation diagram that occurs in the interval $[I_3, I_4] = [7.84, 7.92]$ does not affect the overall behaviour of the solutions of the HH equations. For T above 7.72 °C, the parameters in equations (1) change and the dotted limit cycle curve in figure 2b) loses its one-to-many feature. The chaotic behaviour conjectured in [Guckenheimer and Oliva, 2002] occurs in the interval $[I_3, I_4]$, figure 2b).

However, for $i < I_0$, the HH equations may develop an action potential. In this case, the equations have only one stable fixed point and asymptotically in time all the solutions converge to the steady rest state of the cell/neuron.

3. Type I intermittency in the HH equations

If a cell or neuron is perturbed with some constant transmembrane current $i < I_0$, where I_0 is the parameter value of the SNLC bifurcation, and there is no diffusion $(\tilde{D} = 0)$, the asymptotic time solutions of the HH equations converge to the stable fixed point $x^*(i)$, for any initial condition away from it. In this parameter region $(i < I_0)$, if the initial condition is away from the fixed point, let us say $x_0 = (V_0, n_0, m_0, h_0) \neq x^*(i)$, then the response of the system has two possible outcomes. If x_0 is close enough to $x^*(i)$, then the

asymptotic solutions of the HH equations converge to $x^*(i)$, without ever doing a long excursion through phase space regions away from the fixed point. On the contrary, if x_0 is sufficiently displaced form $x^*(i)$ in the (V, n, m, h) four-dimensional phase space, the solution of the HH equations does a large excursion in phase space, resembling, during some time, an almost periodic orbit — action potential response. These two regions in phase space are separated by a boundary or threshold.

As the parameter i approaches I_0 and x_0 is sufficiently displaced from $x^*(i)$, the larger are the number of transient spikes that appear in the potential V. For the same $i < I_0$, it is possible to produce zero, one, or more spikes, depending on how far x_0 is from $x^*(i)$. There is, however, an upper limit for which, no matter how much we continue to displace x_0 from $x^*(i)$, no more spikes are produced. Thus, there is a maximum number of obtainable spikes for each $i < I_0$. Depending on the value of x_0 , the number of spikes generated must be either equal to or below this maximum. In figure 3, we show this transient behaviour of the solutions of equations (1), for several values of x_0 and fixed $i < I_0$.

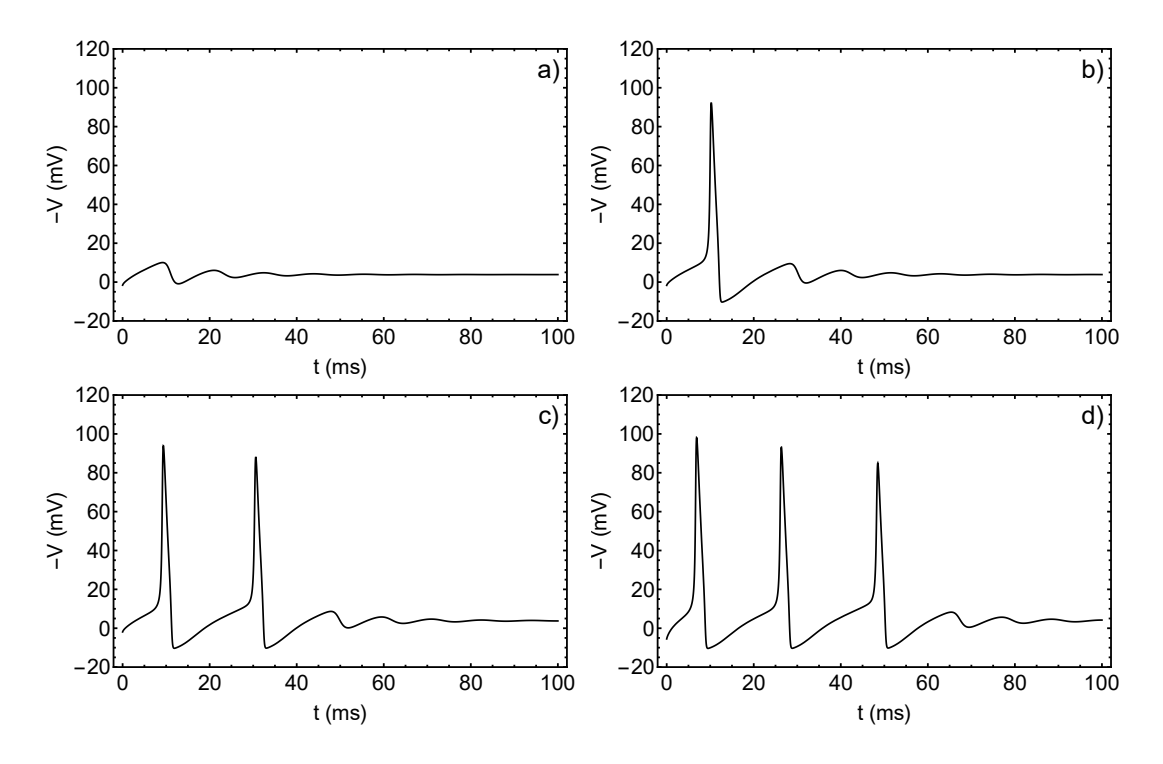


Figure 3. Membrane action potential response of the HH equations (1), for $i = 6.20 < I_0$ and initial conditions $x_0 = (V^*(0) + \Delta V_0, n^*(0), m^*(0), h^*(0))$. a) $\Delta V_0 = 1.6$, b) $\Delta V_0 = 1.7$, c) $\Delta V_0 = 1.9$, and d) $\Delta V_0 = 5.5$. The SNLC bifurcation occurs at $i = I_0 = 6.26$.

As shown in figure 3, the solutions of the HH equations are action potential type responses and, as we shall see now, they are the result of a type I intermittency phenomenon, [Pomeau and Manneville, 1980], [Guckenheimer and Holmes, 2002] and [Dias de Deus et al., 1984], near the codimension 2 SNLC bifurcation. For these

parameter values, the unique attractor in the 4-dimensional phase space is the fixed point $x^*(i)$.

To show that the transient time behaviour shown in figure 3 corresponds to type I intermittency, we analyse the behaviour of the solutions of the HH equations near the SNLC bifurcation at $i = I_0$ (figure 2). At $i = I_0$ and near the fixed point $x^*(I_0)$, the HH equations have a two dimensional center manifold and a two dimensional stable manifold. By the reduction principle, [Kuznetsov, 2004], near the SNLC bifurcation, the asymptotic time solutions of the HH equations are topologically equivalent to the asymptotic time solutions of the normal form for this bifurcation. In fact, the bifurcation diagram in figure 2 is similar to the bifurcation diagram of the codimension 2 Bautin bifurcation, eventually along a parameterised path on a 2-dimensional parameter space, [Kuznetsov, 2004].

With this simple fact, in Appendix A, we show that the intermittency characteristic of the SNLC codimension 2 bifurcation has the same scaling behaviour in the bifurcation parameter as the type I intermittency observed in interval maps, [Pomeau and Manneville, 1980] and [Guckenheimer and Holmes, 2002]. To be more specific, with $\varepsilon = I_0 - i$, the permanence time of the orbits of the HH equations (1) in the vicinity of the limit cycle that appears at the SNLC bifurcation ($\varepsilon = 0$) is $t_{per} = c/\sqrt{\varepsilon}$, where c is a constant. Denoting by P the period of the shadow limit cycle responsible for the spiky action potential response and by N the number of action potential spikes generated before the system goes to the rest steady state, we have $NP = t_{per}$, implying that

$$ln N = C - \frac{1}{2} ln \varepsilon,$$
(3)

where C is a constant (Appendix A).

The first test showing that the action potential solutions of the HH equations are associated with type I intermittency is to verify that the maximum number of action potencial spikes developed in the solution of the HH equations obeys the scaling relation (3).

A second test of type I intermittency is to show that, close to the SNLC bifurcation, the maximum amplitude of each action potential spike, as a function of the maximum amplitude of the previous one, has a parabolic profile. This graph will be called the next amplitude map, [Pomeau and Manneville, 1980].

In figure 4a), we show the number of spikes of the action potential generated by the HH equation, in the left vicinity of the SNLC bifurcation, as a function of $\varepsilon = I_0 - i$. For $\varepsilon \in [0.00030, 0.07532]$, the slope of the fit is s = -0.505, in agreement with the estimate (3). In figure 4b), we calculate the next amplitude map, where we observe the typical parabolic profile associated with type I intermittency.

The main conclusion of this analysis is that the diffusion free $(\tilde{D} = 0)$ HH equations (1) exhibit type I intermittency in the left vicinity of the SNLC bifurcation. This intermittency phenomenon is responsible for the action potential spiky signals. The threshold is associated with a boundary in phase space that separates the two possible

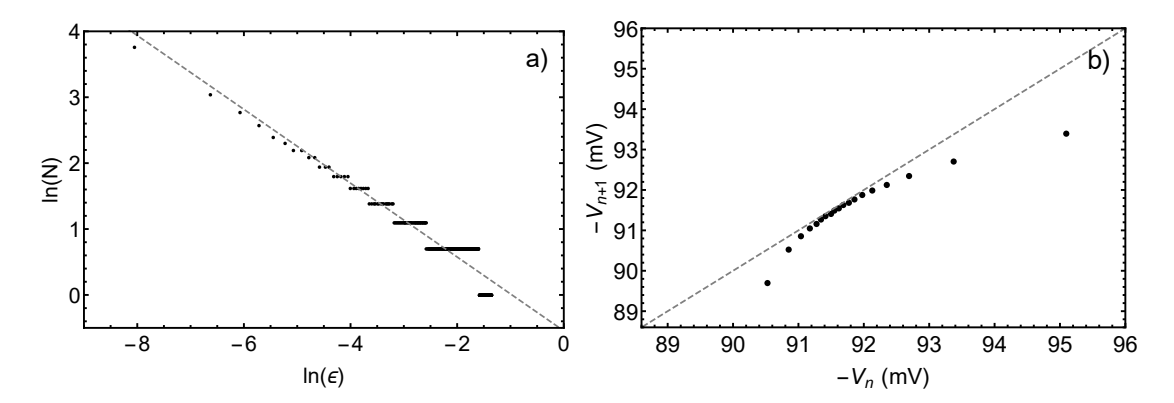


Figure 4. SNLC intermittency for the HH model. a) Logarithm of the number of spikes N of the action potential in the left vicinity of the SNLC bifurcation, as a function of the logarithm of $\varepsilon = I_0 - i$. The slope of the fitted line is s = -0.505, in agreement with (3). b) Next amplitude map for the HH model, for the parameter value i = 6.259, or $\varepsilon = 0.001$. V_N is the maximum value of the action potential spike number N. At the SNLC bifurcation, $\varepsilon = 0$, the parabolic profile shown touches the dotted line $V_{N+1} = V_N$.

types of transient solutions. Our numerical analysis shows that for $i \in [0, I_0)$ and if the electrophysiological state of the cell is sufficiently far from the steady state, the HH model always shows an intermittent response, with one or several action potential spikes.

4. Oscillatory and turbulent solutions of the HH equations

The HH equations (1) with spatial term, D > 0, describe the axonal propagation of the potential function, as well as the opening and closing of ion channels. We consider a 1-dimensional domain of length L representing the axon. In the interior of the spatial domain, there is no membrane current excitation, but at the boundary x = 0 the neuron is excited with some (transmembrane) current i(t). Under these conditions, the HH equations (1) are rewritten in the form

$$\frac{\partial V}{\partial t} = D \frac{\partial^2 V}{\partial x^2} + F(V, \vec{n}) \quad \text{with} \quad x \in (0, L]$$

$$\frac{\partial \vec{n}}{\partial t} = G(V, \vec{n})$$

$$\frac{\partial V}{\partial t} = D \frac{\partial^2 V}{\partial x^2} + F(V, \vec{n}) + \frac{1}{C_m} i(t) \quad \text{with} \quad x = 0,$$
(4)

where i(t) is zero on the first two equations (the excitation signal i(t) only exists for x = 0), x is measured in cm and t in ms. The last three equations in (1) have been collapsed into a single equation in (4). The vector functions F and G are defined by comparison between equations (4) and (1) and $D = \tilde{D}/C_m$. We further consider that the transmembrane potential and the gate variables obey Neumann or zero flux boundary

conditions

$$\frac{\partial V}{\partial x}\Big|_{x=0,L} = 0$$
 and $\frac{\partial \vec{n}}{\partial x}\Big|_{x=0,L} = 0.$ (5)

In Appendix A, it is shown that the diffusion term in (4) does not change the stability of the steady state $x^*(0)$, and the linear analysis leads to the conclusion that the homogeneous steady state of the extended HH equation is stable. However, away from the steady state, the situation can be different.

As the local dynamics of the HH model has intermittent solutions, we analyse numerically how intermittency and diffusion affect the propagation of the action potential along the axon.

To simulate numerically the reaction-diffusion equations (4) we have used a benchmarked numerical method, [Dilão and Sainhas, 1998], obeying the discrete conservation law $\Delta x = \sqrt{6D\Delta t}$, where Δx and Δt are space and time discretisation steps. This relation between space and time steps minimizes the integration error.

For numerical analysis purposes, we have chosen the axon length L=50 cm, with the spatial region divided into M=400 small intervals of length Δx , where $L=M\Delta x$. As $D=\Delta x^2/(6\Delta t)=L^2/(6M^2\Delta t)$, we change Δt in the interval [0.003, 0.033] ms, which corresponds to variations in the diffusion coefficient in the interval [0.23, 2.34] cm²/ms. The value suggested by Hodgkin and Huxley, [Hodgkin and Huxley, 1952], is $\tilde{D}=3.4\times~10^{-4}~\rm S$, giving $D=0.34~\rm cm^2/ms$, which is within the range of our numerical analysis.

To analyse the solutions of the extended HH equations (4), we have imposed a constant signal $i(t)=i_0$, for every $t\geq 0$, at x=0 The initial condition along the axon was set to $x^*(0)=(V^*(0),n^*(0),m^*(0),h^*(0))$. According to the parameters described above, we have varied the diffusion coefficient in the realistic range $D\in [0.23,2.34] \text{ cm}^2/\text{ms}$. In this range of the diffusion coefficient, $D/\Delta x^2\in [5,50] \text{ ms}^{-1}$.

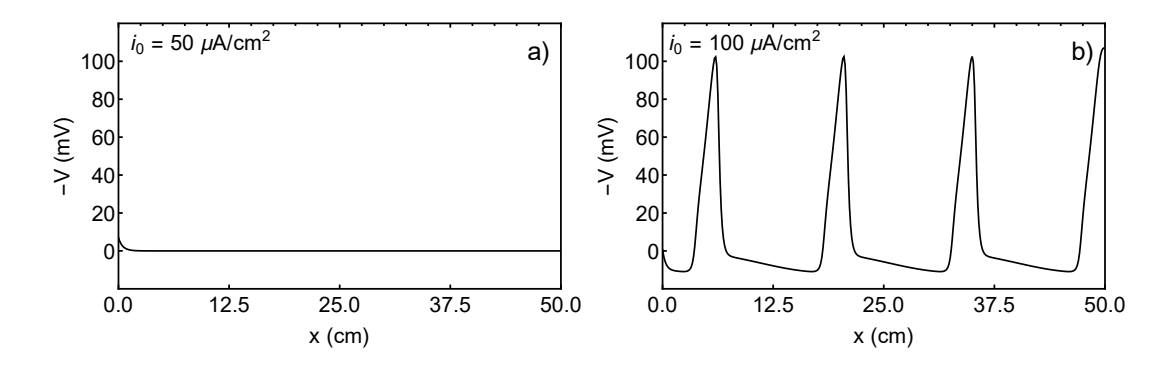


Figure 5. Spatial solutions of the HH equations (4), for $D/\Delta x^2 = 20 \text{ ms}^{-1}$ at time t = 100 ms, for two different values of the transmembrane current. In a), $i_0 = 50 \,\mu\text{A/cm}^2$ and the transmembrane potential converges to the steady state $x^*(0)$ along the axon. In b), $i_0 = 100 \,\mu\text{A/cm}^2$ and the transmembrane potential develops a propagating periodic action potential.

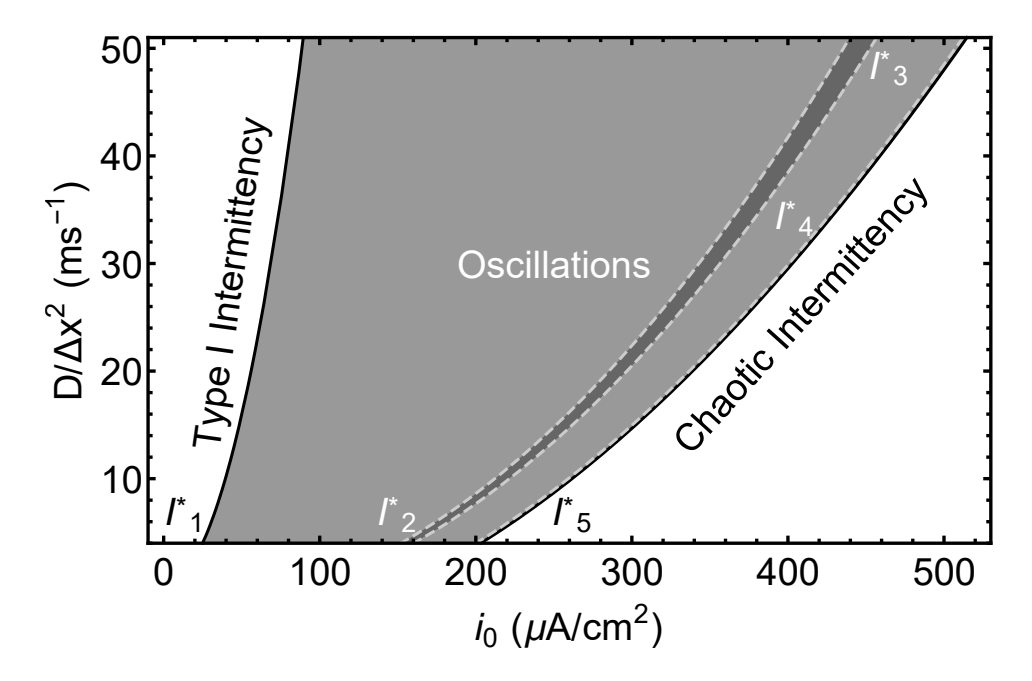


Figure 6. Bifurcation diagram of the HH extended model (4), as a function of the transmembrane current i_0 at the axon boundary and of the diffusion coefficient $D/\Delta x^2$. We show two different types of intermittency, oscillations and spatial chaos (dark grey and dotted lines).

In figure 5, we show that we can have sustained oscillations as a result of the intermittency effect of the diffusion free HH equations for i = 0. If the input transmembrane current at the axon boundary is low, for example $i_0 = 50 \ \mu\text{A/cm}^2$, the resulting transmembrane potential along the axon converges to the steady state $x^*(0)$, in agreement with the stability analysis in Appendix A. If the input transmembrane current at the axon boundary is above some threshold, stable oscillations develop.

Further numerical simulations have shown that, for a certain range of the parameter i_0 , the extended HH system (4) has spatial intermittency and periodic oscillations. In figure 6, we depict in the $(i_0, D/\Delta x^2)$ parameter space, the regions where both phenomena are observed. This result shows that the extended HH system has some attractor set other than the homogeneous fixed point $x^*(0)$.

In figure 6, the black lines I_1^* and I_5^* delimit the regions where equations (4) show solutions with intermittency from regions with oscillatory and chaotic solutions. For parameters in the intermittency regions, the solutions of equations (4) show a finite number of spikes along the spatial domain before going to the stable steady state. The light grey region marks the solutions that are oscillatory and propagate through the spatial region (figure 5b)). Between the light dashed lines I_2^* and I_3^* the time interval between successive spikes is irregular — dark grey region. The light dashed line I_4^* precedes the final line I_5^* only by a couple of decimal places and marks the beginning of a chaotic region, characterised by the chaotic behaviour of the time interval between successive action potential spikes (figure 7c)). The chaotic region ends giving rise to

what we call chaotic intermittency. Type I intermittency and chaotic intermittency will be analysed in more detail in the next subsections.

In figure 7, we make a detailed bifurcation analysis along a cross section of the bifurcation diagram in figure 6, for the diffusion coefficient $D/\Delta x^2 = 20 \text{ ms}^{-1}$ and spanning the whole region $[I_1^*, I_5^*]$. In this figure, the period of oscillations as a function of the transmembrane current i_0 is plotted. Figure 7a) shows the whole region, while figures 7b) and 7c) are different zoom ins of the bifurcation diagram. As shown, regular oscillations occur in the regions $[I_1^*, I_2^*]$ and $[I_3^*, I_4^*]$ and there are complex bifurcations or chaotic regions in the intervals $[I_2^*, I_3^*]$ and $[I_4^*, I_5^*]$. In the regions, $[I_2^*, I_3^*]$ and $[I_4^*, I_5^*]$, the time intervals are irregular and show a bifurcation pattern characteristic of chaotic maps of the interval (figure 7c)).

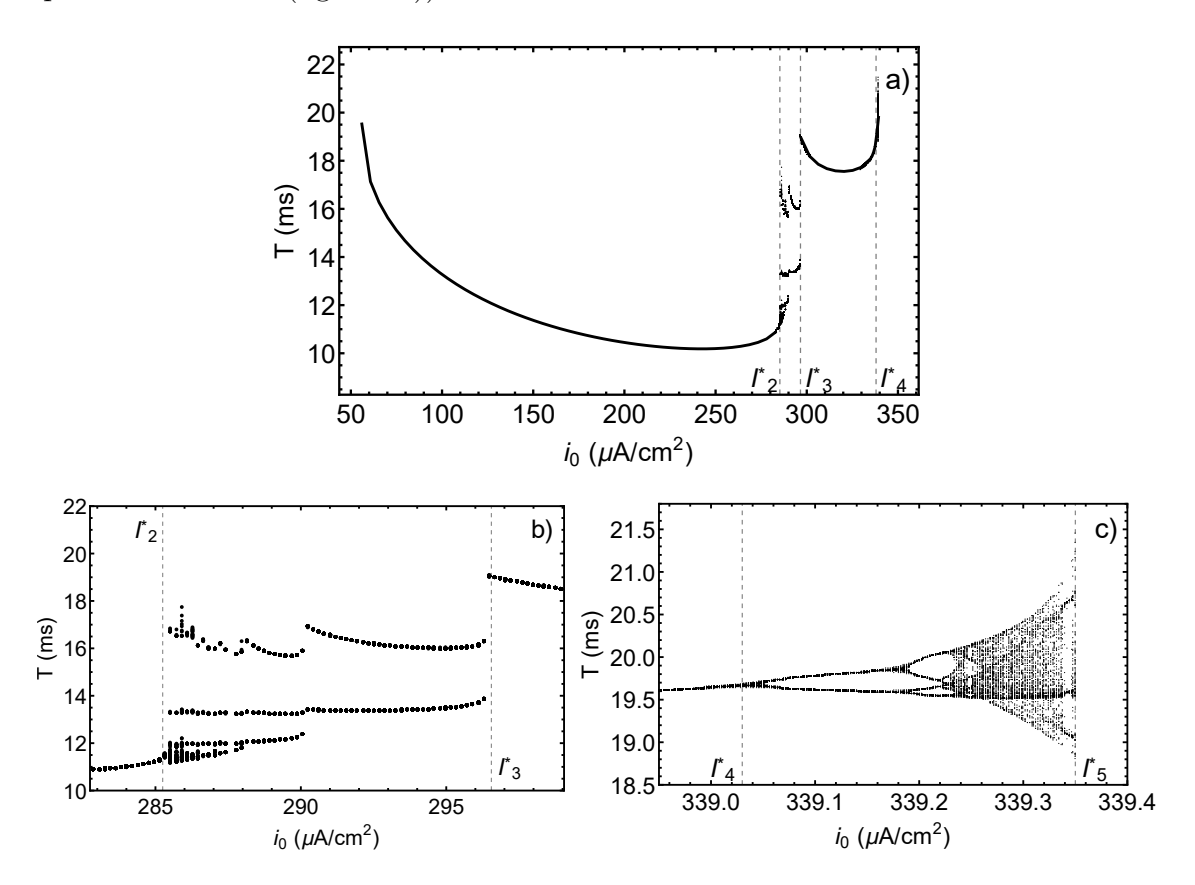


Figure 7. a) Period (and time intervals) of the oscillatory solutions of the HH extended model (4), as a function of the current i_0 , for the diffusion coefficient $D/\Delta x^2 = 20 \text{ ms}^{-1}$. In the regions $[I_2^*, I_3^*]$ (b) and $[I_4^*, I_5^*]$ (c), the solutions of the HH extended model show chaos.

We have calculated the velocity of propagation of the action potentials for different values of the diffusion coefficient. The numerical values are shown in figure 8. These results are of the same order of magnitude of the experimental velocity v = 21.2 m/s measured by Hodgkin and Huxley in the giant axon of the squid *Loligo*, [Hodgkin and Huxley, 1952].

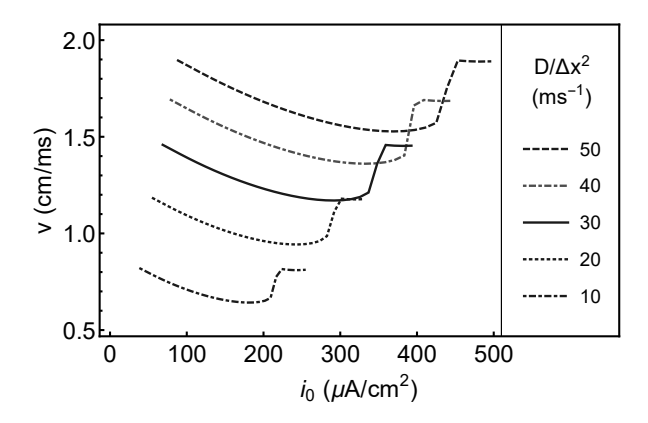


Figure 8. Wave velocity of the action potential for five different diffusion coefficients of the HH equations (4), in the parameter region $[I_1^*, I_5^*]$.

4.1. Type I spatial intermittency

In the region $i_0 < I_1^*$ of figure 6, the HH model with diffusion has type I intermittency solutions. To characterise this intermittency, we have tested the parameter scaling and the next amplitude map as in section 3. In the intermittency regime, we have counted the number of action potential spikes that propagate along the domain [0, L], and have calculated the next amplitude maps. In figure 9 we show the analogous of figure 4, now for the spatial HH equations, with $\varepsilon = I_1^* - i_0$ in the domain $\varepsilon \in [0.001, 0.231]$. The numerically determined slope of the scaling relation (3) is s = -0.506, in agreement with the theoretical prediction s = -0.5. The next amplitude map has been calculated for $i_0 = 56.010 < I_1^* = 56.012$ and $D/\Delta x^2 = 20$ cm⁻¹, showing a parabolic profile, characteristic of type I intermittency.

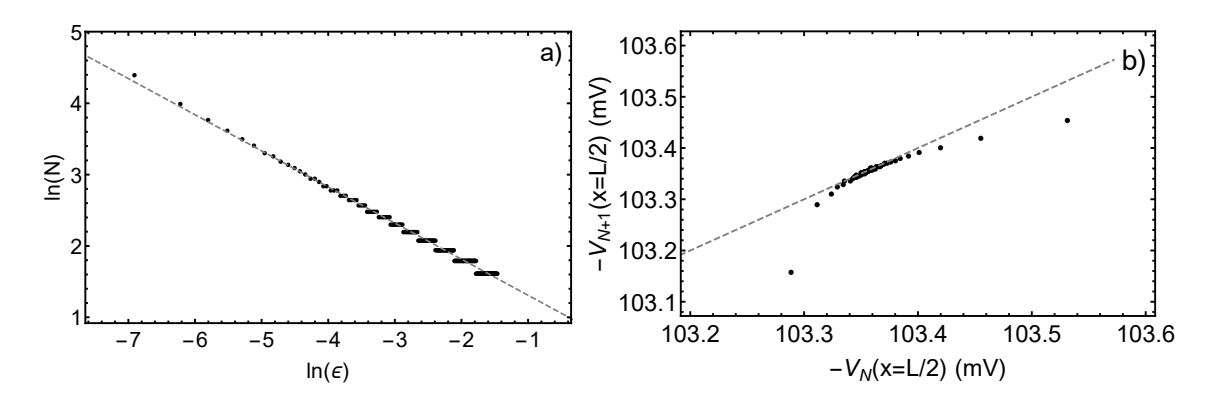


Figure 9. Type I intermittency for the HH extended model (4), with $D/\Delta x^2 = 20 \text{ cm}^{-1}$. a) Logarithm of the number of spikes N of the action potential in the left vicinity of $I_1^* = 56.012$. The slope of the fitted dotted line is s = -0.506, in good agreement with (3). b) Next amplitude map for the parameter value $i_0 = 56.010$ or $\varepsilon = 0.002$. $V_N(x = L/2)$ is the maximum value of the action potential spike number N, measured at the middle of the spatial domain [0, L]. The dotted line is the graph of the equation $V_{N+1} = V_N$.

4.2. Chaotic intermittency

Chaotic intermittency of the HH extended model appears for $i_0 > I_5^*$. In this case, the solutions of the HH extended model converge to the stable steady state $x^*(0)$, but the transient solution has a finite sequence of action potential spikes with variable time intervals between spikes. This intermittent behaviour in the transient process and the number of spikes depends on the initial condition and on the distance to I_5^* , without showing any scaling relations. In figure 10, we show the logarithm of the number of spikes as a function of the bifurcation parameter $\varepsilon = i_0 - I_5^*$, and the next amplitude map for the parameters $i_0 = 339.369$, with diffusion coefficient $D/\Delta x^2 = 20$ cm⁻¹. From figure 10a), we conclude that the intermittent behaviour has no apparent scaling and is different from other types of intermittency. On the other hand, the number of spikes as a function of the distance ε to the bifurcation point seems to behave randomly, without any scaling behaviour. Also, the next amplitude map shown in figure 10b) is not characteristic of any type of known intermittency phenomenon.

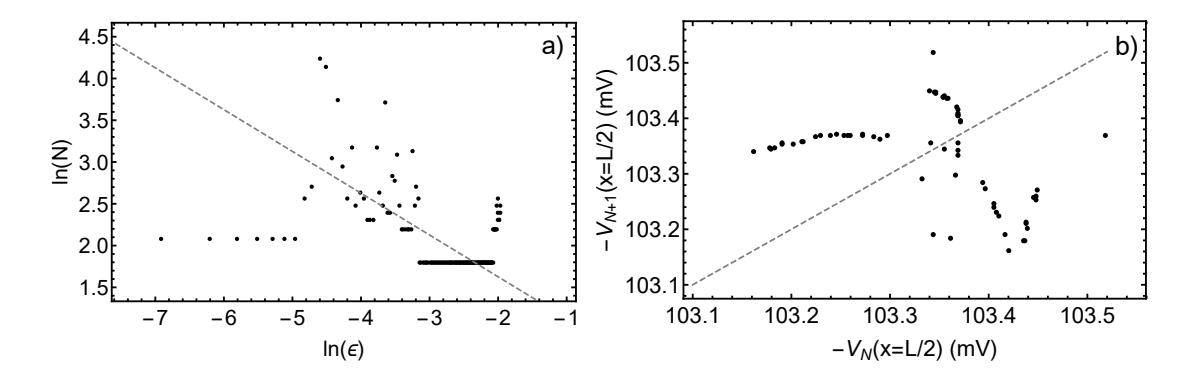


Figure 10. Chaotic intermittency for the HH extended model (4), with $D/\Delta x^2 = 20 \text{ cm}^{-1}$. a) Logarithm of the number of spikes N of the action potential in the right vicinity of I_5^* , for $\varepsilon = i_0 - I_5^* \in [0.001, 0.140]$. The dotted line has slope s = -0.5. b) Next amplitude map for the parameter value $i_0 = 339.369$ or $\varepsilon = 0.010$. $V_N(x = L/2)$ is the maximum value of the action potential spike number N, measured at the middle of the spatial domain [0, L]. Chaotic intermittency does not show any scaling behaviour on the number of spikes as a function of ε . The dotted line is the graph of the equation $V_{N+1} = V_N$.

5. Discussion

We have found the geometric and dynamical origins of the action potential type response of the Hodgkin-Huxley neuron model. This peculiar response is due to type I intermittency occurring in the vicinity of a saddle-node bifurcation of limit cycles. In this regime, neurons have a stable steady state but for large amplitudes of excitation they develop the action potential type of response, shadowing the existence of a stable limit cycle that appears at different parameter values. These conclusions

were obtained under zero diffusion, implying that our results remain true for any cell with an electrophysiological state controlled by voltage sensitive channels.

We have extended our analysis to neurons with long axons. In this case, the diffusion coefficient of the HH model is positive and the solutions of the HH model equations show a more complex behaviour. For this case, we have assumed that neuron excitation is done at one boundary of the spatial domain through a transmembrane current. We have shown that, above some transmembrane current threshold, action potentials spikes develop, showing type I intermittency characterised by a finite number of action potential spikes propagating along the axon. Increasing the values of the transmembrane current at the boundary of the axon, periodic propagating stable diffusion waves along the axon appear. In the parameter range of oscillations, we may have turbulent oscillations or chaos. These chaotic oscillations appear on the irregular time interval between successive action potential spikes and have a bifurcation diagram similar to the ones found in interval maps (figure 7c)). For the parameter values where oscillatory or chaotic solutions exist, the steady state of the HH equations remains stable and is reached for small values of transmembrane currents at the axon boundary.

As far as we know, this is the first time that intermittency phenomena, chaotic or type I, are reported in an electrophysiological model of a cell. However, it is a common phenomenon found in electroencephalogram, [Rae-Grant and Kim, 1994], and epilepsia, [Velazquez et al., 1999].

Our analyses have been done for the original and calibrated HH model equations (1) and (4), with realistic diffusion coefficients. This implies that all the phenomena described here are predictions that can be explored in patch clump experiments on giant axons. All the simulations are in agreement with HH observations, including the velocity of propagation of action potentials measured along the *Loligo* giant axon.

Acknowledgments

One of the authors (RD) would like to thank IHÉS for its hospitality and Simons Foundation for support.

Appendix

Intermittency near a SNLC bifurcation

The normal form of the Bautin bifurcation in polar coordinates is ([Kuznetsov, 2004])

$$\begin{cases} \dot{r} = r(\beta_1 + \beta_2 r^2 - r^4) = f(r) \\ \dot{\phi} = 1, \end{cases}$$
 (6)

where β_1 and β_2 are real parameters. A simple analysis shows that, if $\beta_2 > 0$ and $\beta_1 < 0$, there is a saddle node bifurcation in the radial variable r, which corresponds to a SNLC bifurcation in the cartesian coordinates. The codimension 2 SLNC bifurcation occurs

for $\beta_1 = \beta_1^* = -\beta_2^2/4$ and a limit cycle is created with radial coordinate $r^* = \sqrt{\beta_2/2}$. We take now the new parameter ε defined by

$$\beta_1 = -\frac{1}{4}\beta_2^2 - \varepsilon. \tag{7}$$

For $\beta_2 > 0$, the system of equations (6) has a SNLC bifurcation for $\varepsilon = 0$. If $\varepsilon > 0$, the system of equations (6) has no limit cycles and, if $\varepsilon < 0$, the system of equations (6) has two limit cycles with radial coordinates $r_{\rm S} = \sqrt{(\beta_2 + \sqrt{-\varepsilon})/2}$ and $r_{\rm U} = \sqrt{(\beta_2 - \sqrt{-\varepsilon})/2}$, where the subscripts "s" and "u" stand for stable and unstable, respectively.

Along any line $\beta_2 = \text{constant}$ with $\beta_2 > 0$, for $\varepsilon < 0$, the asymptotic solutions of equation (6) with initial condition $r_0 > r_s$ converge to a stable limit cycle. For $\varepsilon > 0$ but close to zero, the graph of y = f(r) has a local maximum near $r_{max} = \sqrt{\beta_2/2}$ which is very close to the line y = 0. For initial conditions $r_0 > r_s$ and by the continuity of the solutions of the differential equation in order to ε , the radial solution of equation (6) will be near $r = r_{max}$ for a long interval of time. This interval of time goes to infinity, as $\varepsilon \to 0$. So, during this period of time, the solution of the differential equation will resemble the solution along a limit cycle that does not exist. This is the phenomenon of type I intermittency, [Pomeau and Manneville, 1980] and [Guckenheimer and Holmes, 2002].

As a function of ε , we estimate the time of permanence of the solution of equation (6) near the point $r_{max} = \sqrt{\beta_2/2}$, the radius of the limit cycle at bifurcation. As this analysis is local, we take $u = r - r_{max}$ and, by (7), the first equation in (6) is rewritten as

$$\dot{u} = -\varepsilon (r_{max} + u) - \sqrt{2}\beta_2^{3/2} u^2 + \mathcal{O}(u^3) = g(u) + \mathcal{O}(u^3). \tag{8}$$

In this new coordinate, the SNLC bifurcation occurs for $\varepsilon = 0$ and the limit cycle has u-radial coordinate $u = r - r_{max} = 0$.

For an initial condition u(0) = d > 0, the time of permanence of the solutions of equation (8) in the interval [-d, d] is

$$t = \int_{-d}^{d} \frac{du}{g(u)} = \frac{2}{\sqrt{\varepsilon}} \frac{1}{\sqrt{4\beta_2^2 - \varepsilon}} \arctan \frac{\varepsilon + 2\sqrt{2}u\beta_2^{3/2}}{\sqrt{\varepsilon}\sqrt{4\beta_2^2 - \varepsilon}} \bigg|_{-d}^{d}.$$
 (9)

In the limit $\varepsilon \to 0$, $\arctan(.) \to \pi/2$ and the previous expression becomes

$$t = \frac{\pi}{\beta_2 \sqrt{\varepsilon}}. (10)$$

Thus, we have proved that in the left vicinity of a codimension 2 SNLC bifurcation, the orbits follow a trajectory ressembling a limit cycle oscillation during a time that goes to infinity as the bifurcation is approached.

Stability of the steady state of the HH equations

Here, we analyse the stability of the homogeneous stable state $x^*(0) = (V^*(0), n^*(0), m^*(0), h^*(0))$ of the first and third equations in (4), with the boundary conditions (5).

Due to the zero flux boundary conditions (5), the solutions of the first and third equations in (4) can be written in the form

$$V(x,t) = V^{*}(0) + \sum_{k\geq 1} a_{k}(t) \cos 2\pi kx/L$$

$$n(x,t) = n^{*}(0) + \sum_{k\geq 1} b_{k}(t) \cos 2\pi kx/L$$

$$m(x,t) = m^{*}(0) + \sum_{k\geq 1} c_{k}(t) \cos 2\pi kx/L$$

$$h(x,t) = m^{*}(0) + \sum_{k\geq 1} d_{k}(t) \cos 2\pi kx/L,$$
(11)

where $a_k(t)$, $b_k(t)$, $c_k(t)$ and $d_k(t)$ are time dependent unknown functions of time, and V(x,t), n(x,t), m(x,t), $h(x,t) \in L^2([0,L])$, for every $t \geq 0$. As usual, $a_k(t)$, $b_k(t)$, $c_k(t)$ and $d_k(t)$ are the k-eigenmode solutions of the extended HH equations. To analyse the stability of $x^*(0)$, following [Dilão, 2005], we introduce (11) into the first equation in (4) and, up to first order in the phase space variables we obtain

$$\begin{pmatrix}
\dot{a}_{k} \\
\dot{b}_{k} \\
\dot{c}_{k} \\
\dot{d}_{k}
\end{pmatrix} = \begin{pmatrix}
\frac{\partial F}{\partial V} - D \frac{4\pi^{2}k^{2}}{L^{2}} & \frac{\partial F}{\partial n} & \frac{\partial F}{\partial m} & \frac{\partial F}{\partial h} \\
\frac{\partial G_{n}}{\partial V} & \frac{\partial G_{n}}{\partial n} & 0 & 0 \\
\frac{\partial G_{m}}{\partial V} & 0 & \frac{\partial G_{m}}{\partial m} & 0 \\
\frac{\partial G_{h}}{\partial V} & 0 & 0 & \frac{\partial G_{h}}{\partial h}
\end{pmatrix} \begin{pmatrix}
a_{k} \\
b_{k} \\
c_{k} \\
d_{k}
\end{pmatrix}, (12)$$

for every $k \geq 1$ and the matrix is evaluated at $x^*(0)$. If, for every k > 1, the real parts of the eigenvalues of the jacobian matrix in equation (12) are negative, the homogeneous spatial solution $(V(x,t),\vec{n}(x,t)) = x^*(0)$ of the first and third equations in (4) is stable. Due to the complex form of the vector field components, the jacobian matrix is difficult to calculate. So, we have analysed numerically the real part of its eigenvalues, for a large range of the index k. For values of the eigenmode number k, up to k = 2000, and for $D \in [10^{-6}, 10]$, all the eigenvalues of the matrix in (12) have negative real parts, implying that the homogeneous steady state of the extended HH equation is stable.

References

[Keener and Sneyd, 1998] Keener, J. P. and Sneyd, J., Mathematical physiology, Springer, 1998.
[Hodgkin and Huxley, 1952] Hodgkin, A. L. and Huxley, A. F., A quantitative description of membrane current and its application to conduction and excitation in nerve, J. Physiol. 117 (1952) 500-544.
[Hodgkin and Huxley, 1952b] Hodgkin, A. L. and Huxley, A. F., The components of membrane conductance in the giant axon of Loligo, J. Physiol. 116 (1952) 473-496.

[Rinzel and Miller, 1980] Rinzel, J. and Miller, R. N., Numerical Calculation of Stable and Unstable
 Periodic Solutions to the Hodgkin-Huxley Equations, Mathematical Biosciences 49 (1980) 27–59.
 [Izhikevich, 2007] Izhikevich, E. M., Dynamical systems in neuroscience, MIT press, 2007.

- [Ermentrout and Terman, 2010] Ermentrout, G. B. and Terman, D. H., Mathematical foundations of neuroscience, Springer, 2010.
- [Rae-Grant and Kim, 1994] Rae-Grant, A. D. and Kim, Y. W., Type III intermittency: a nonlinear dynamic model of EEG burst suppression, Electroencephalography and clinical Neurophysiology, 90 (1994) 17-23.
- [Velazquez et al., 1999] Velazquez, J. L. P., Khosravani, H., Lozano, A., Bardakjian, B. L., Carlen, P. L. and Wennberg, R., Type III intermittency in human partial epilepsy, European Journal of Neuroscience, 11 (1999) 2571-2576.
- [Hassard, 1978] Hassard, B., Bifurcation of Periodic Solutions of the Hodgkin-Huxley Model for the Squid Giant Axon, J. Theor. Biol. 71(1978) 401-420.
- [Guckenheimer and Oliva, 2002] Guckenheimer, J. and Oliva, R. A., Chaos in the Hodgkin-Huxley Model, SIAM J. Applied Dynamical Systems, 1 (2002) 105-114.
- [Doedel et al., 1991] Doedel, E., Keller, H. B. and Kernévez, J. P., Numerical analysis and control of bifurcation problems I, Internat. J. Bifur. Chaos, 1 (1991) 493–520.
- [Ermentrout, 2002] Ermentrout, B., Simulating, analyzing, and animating dynamical systems: A Guide to XPPAUT for researchers and students, SIAM 2002, Philadelphia, USA.
- [Kuznetsov, 2004] Kuznetsov, Y. A., Elements of applied bifurcation theory, third edition, Springer, Berlin, 2004.
- [Pomeau and Manneville, 1980] Pomeau, Y. and Manneville, P., Intermittent transition to turbulence in dissipative dynamical systems, Comm. Math. Phys. 74 (1980) 189–197.
- [Guckenheimer and Holmes, 2002] Guckenheimer, J. and Holmes, P., Nonlinear Oscillations, Dynamical Systems, and Bifurcations of Vector Fields, Springer, 2002.
- [Dias de Deus et al., 1984] Dias de Deus, J., Dilão, R. and Noronha da Costa, A., Intermittency and sequences of periodic regions in one dimensional maps of the interval, Physics Letters A, 101 (1984) 459-463.
- [Dilão and Sainhas, 1998] Dilão, R. and Sainhas, J., Validation and Calibration of Models for Reaction-Diffusion Systems, International Journal of Bifurcation and Chaos, 8 (1998) 1163-1182.
- [Dilão, 2005] Dilão, R., Turing Instabilities and Patterns Near a Hopf Bifurcation, Applied Mathematics and Computation, 164 (2005) 391-414.